HEFAT2014
10th International Conference on Heat Transfer, Fluid Mechanics and Thermodynamics
14 – 26 July 2014
Orlando, Florida

ANALYTICAL STUDY OF FLOW AND HEAT TRANSFER IN CROSS AND NON CROSS FLOW JET PLATE SOLAR AIR HEATER

Singh S N * and Nayak Rajen Kumar
* Author for correspondence
Department of Mechanical Engineering,
ISM Dhanbad,
Jharkhand
India,
E-mail: snsingh631@yahoo.com

ABSTRACT

This paper presents an analytical study of flow and heat transfer in cross and non - cross flow solar air heater for inline and staggered plates inserted between absorber and bottom plates. Results are presented for various parameters of cross and non - cross flow such as pitch to hole diameter of the jet plate (X / D = 6.0 – 10.0), height of the upper channel to hole diameter (Z_1 / D = 6.0 – 10.0), height of the lower channel to hole diameter (Z_2 / D = 8.0 - 14.0), Reynolds number (Re = 3000 - 43000), In this study, heat transfer coefficient, outlet temperature of air, collector efficiency and friction factor are calculated for the above parameters. In a cross - flow inline hole jet plate solar air heater, the considerable increment in collector efficiency has been found from 15.68 to 54.88% for $\dot{m}_1$ = 50 – 300 kg / hm^2, X / D = 6.0 - 10.0 and N = 561 whereas the value of heat transfer coefficient is increased from 3.24 to 8.40 W/m^{2}K for X / D = 6.0 - 10.0 and $\dot{m}_1$ = 50 kg/hm^2 which is higher than cross - flow staggered hole and non - cross flow inline/staggered hole jet plate solar air heater. The Nusselt number (Nu) increase with decrease in jet hole diameter (D) for fixed mass flow rate.

INTRODUCTION

In recent times, there has been a renewed interest in non conventional jet plate solar air heater because of having better performance with compared to a conventional solar air heater.

Several configurations of absorber plates are designed to improve the performance of a conventional solar air heater. By providing artificial roughness obstacles, baffles in various shapes with different arrangements and longitudinal fins over and underside [1], of the absorber plate were employed to increase the surface area of the absorber plate. As a result, the heat transfer co-efficient between the absorber plate and the air pass have been increased [2, 3, 4]. On other hand heat transfer

NOMENCLATURE

A	[m^2]	Surface area of absorber plate
A_e	[m^2]	Effective heat transfer area of jet plate
C	[Wh / kg^{o}C]	Specific heat capacity of air, d Air thicness between absorber and cover
D_1, D_2	[m]	Hydraulic diameter $D_1 = \frac{4\ W\ Z_1}{2(w + Z_1)}$, $D_2 = \frac{4\ W\ Z_2}{2(w + Z_2)}$
D	[m]	Diameter of jet hole
f_s		Friction factor
F_1		Dimenssionless constant
F_2		Cross-flow degration factor
g	[m / s^2]	Accelaration due to gravity
G_1	[kg / hm^2]	Mass flow velocity of air impinging out of holes
G_2	[kg / hm^2]	Mass flow velocity of cross - flow air
Gr_c		Grashof number $= \frac{g\ \beta\ (T_P - T_C)d^3}{\nu^2}$
h_{cS}	[W/m^{2}K]	Heat transfer coefficient of cover plate to surrounding air
h_{PC}	[W/m^{2}K]	Heat transfer coefficient of absorber to the cover plate
h_{cPC}	[W/m^{2}K]	Convective heat transfer coefficient of absorber plate to cover plate
h_{cja1}	[W/m^{2}K]	Convective heat transfer coefficient of jet plate to lower channel air
h_{cja2}	[W/m^{2}K]	Convective heat transfer coefficient of jet plate to upper channel air
h_{cba1}	[W/m^{2}K]	Convective heat transfer coefficient of bottom plate to lower channel air
h_{rcs}	[W/m^{2}K]	Radiative heat transfer coefficient of cover plate to surrounding air
h_{rjb}	[W/m^{2}K]	Radiative heat transfer coefficient of jet plate and bottom plate
h_w	[W/m^{2}K]	Coefficient of wind related heat transfer coefficien
h_{rpj}	[W/m^{2}K]	Radiative heat transfer coefficient between absorber and jet plate
h_{Pa2}	[W/m^{2}K]	Heat transfer coefficient of absorber plate to upper channel air
h_{Pj}	[W/m^{2}K]	Average heat transfer coefficient of absorber plate to jet air

h_{CPa2}	[W/m^{2}K]	Convective heat transfer coefficient of absorber plate to upper channel air
I	[W/m^2]	incident solar flux
K_a	[W/mK]	Thermal conductivity of air flowing through channel
l	[m]	Insulation thickness
L	[m]	Collector length
m		Dimension constant
$\dot{m}_1$	[kg / hm^2]	Mass flow rate of air
$\dot{m}_2$	[kg / hm^2]	Mass flow rate of cross - flow air
N		Total number of jet holes on jet plate
N_1	[m]	Height of jet hole
Nu		Nusselt number
Nu_{ja1}		Nusselt number at lower channel
Nu_{ja2}		Nusselt number at upper channel
Nu_{Pj}		Nusselt number between absorber and jet plate
Pr		Prandtl number
Re		Flow Reynolds number
Re_{ja1}		Flow Reynolds number between jet plate and bottom plate
Re_{ja2}		Flow Reynolds number between absorber Plate and jet plate
T_A	[^{o}C]	Ambient temperature
T_{a1}	[^{o}C]	Air temperatur at lower channel
T_{a2}	[^{o}C]	Air temperatur at upper channel
T_b	[^{o}C]	Bottom plate temperature
T_C	[^{o}C]	Glass cover plate temperature
T_i	[^{o}C]	Inlet air temperature above jet plate in mixing of air
T_j	[^{o}C]	Jet plate temperature
T_o	[^{o}C]	Outlet air temperature
T_{ol}	[^{o}C]	Outlet air temperature at jet hole
T_P	[^{o}C]	Absorber plate temperature
T_S	[^{o}C]	Sky temperature
U_b	[W/m^{2}K]	Bottom loss coefficient
V	[m/s]	Jet air velocity
V_w	[m/s]	Wind velocity
X	[m]	Span - wise pitch of jet holes
Y	[m]	Stream - wise pitch of jet holes
Z	[m]	Space between absorber and back plate (in jet plate heater)
Z_1	[m]	Distace between the absorber plate and jet plate
Z_2	[m]	Distance between the jet plate and bottom plate
W	[m]	Air heater width

Greek symbols

α		Solar absrptivity of absorber plate
τ		Reflectivity of glass cover plate
β	[K^{-1}]	Coefficient of thermal expansion
σ	[W/m^2 K^4]	Stefan Boltzman constant,
η	[-]	Collector efficiency
ρ	[kg / m^3]	Density of air
μ	[Pa.s]	Dynamic viscosity of air
ν	[m^2 / s]	Kinematic viscosity of air,
ε_R		Thermal emittance of surface R

Subscripts

a	Air flowing through collector
b	Bottom plate
c	Cover plate
i	Inlet air at upper channel
j	jet air / jet plate
o	Outlet air at heater exit
ol	Outlet air at jet hole
P	Absorber plate
S	Sky

area is increased by providing double pass solar air heater with fin attached [5] jet plate between the absorber plate and bottom plate [6], and flat plate solar air heater consisting one or more glass covers with the air flowing over and under [6, 7, 8, 9]. Hence, their effects in performance of conventional solar air heaters are improved.

The various investigations have been made for improving the heat transfer coefficient in a solar collector by introducing forced convection [10,11], extended heat transfer area [12, 13], and increased air turbulence [12, 14]. Choudhury [15], have evaluated the gain in temperature increment and performance efficiency of the jet concept air heater over that of the parallel plate air heater. With duct depth 10.0 cm, length 2.0 m and air flow rates in the range of 50 to 250 Kg/hm^2, the gain in temperature increment and efficiency are found as 2.5^{o}C and 19.0% respectively. Singh [16], analytically presented the heat transfer enhancement in a continuous longitudinal fins solar air heater for different pitches. Irfan [17], has studied the solar air heater with free and fixed fins and found increased heat transfer coefficient and output air stream temperature. Belusko et al [18], have investigated the improvement on heat transfer coefficient by providing a jet impingement in unglazed air collector. Chauhan et al [19], have suggested on heat transfer coefficient and friction factor correlations for impinging jet solar air heater.

Based on the critical review of the above literatures, it clearly shows that a very few works have been done in the proposed area and to the best of our knowledge performance of a solar air heater with staggered hole jet plate has not been examined so far. Hence the objectives of the present problem to check the influence of inline/staggered hole on the performance of cross and non- cross flow solar air heater.

MATHEMATICAL ANALYSIS

A schematic view of jet plate solar air heater is shown in Fig. 1 which has blower for supplying air, bottom plate, jet plate with inline/staggered hole (shown in Figs. 2 and 3), black painted absorber plate, toughened glass cover plate, two flow -

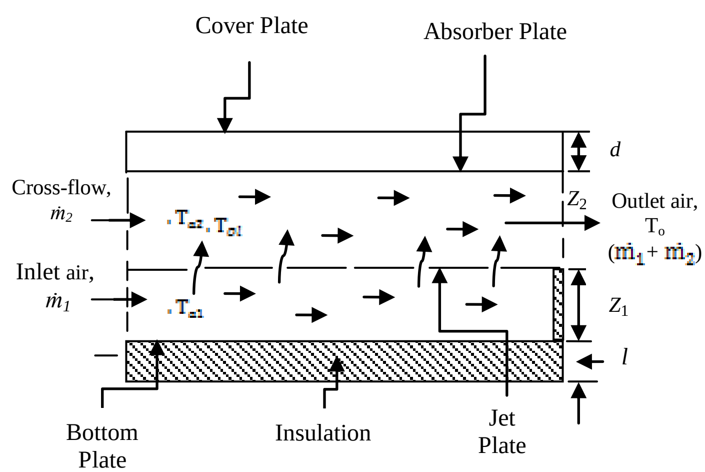

Fig.1. A schematic view of jet plate solar air heater

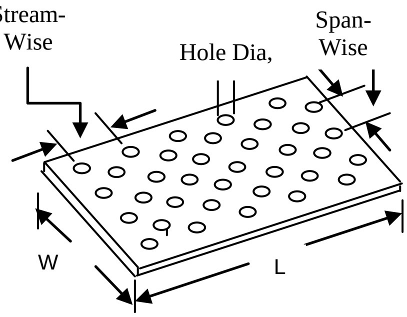

Fig.2. Staggered hole Jet plate

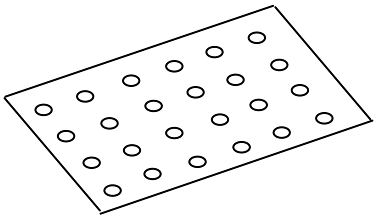

Fig.3. Inline hole Jet plate

channels with the mass flow rate of air $\dot{m}_1$ and $\dot{m}_2$, bottom insulation and thermocouples imbedded to each plate. In case of cross-flow condition, mass flow rate of air between jet plate and bottom plate ($\dot{m}_1$) impinges out of the hole and mixes with $\dot{m}_2$ as shown in Fig. 1 and subsequently the same comes out from the upper channel exit. Under non–cross flow condition, since inlet of upper channel is closed so air from the bottom channel passes through the holes and strikes the lower surface of the absorber plate, finally comes out from the upper channel exit

Energy Balance Equations under Steady State Conditions [15]:

The steady state energy balance equations for the cover, absorber plate, jet plate, back plate, air passage between jet plate and bottom plate and absorber plate and jet plate are written as:

For cover plate,

$$h_{CS}\,(T_C - T_A) = h_{PC}\,(T_P - T_C) \qquad (1)$$

For absorber plate,

$$I\tau\alpha = h_{PC}\,(T_P - T_C) + h_{CPa2}\,(T_P - T_{a2}) + h_{rpj}\,(T_P - T_j) \qquad (2)$$

For jet plate,

$$h_{rpj}\,(T_P - T_j) = h_{cja2}(T_j - T_{a2}) + h_{cja1}(T_j - T_{a1}) + h_{rjb}(T_j - T_b) \qquad (3)$$

For bottom plate,

$$h_{rjb}(T_j - T_b) = h_{cba1}(T_b - T_{a1}) + U_b(T_b - T_A) \qquad (4)$$

For air stream between jet plate and bottom plate,

$$\dot{m}_1\, C(T_{ol} - T_A) = h_{cja1}(T_j - T_{a1}) + h_{cba1}(T_b - T_{a1}) \qquad (5)$$

For air stream between absorber plate and jet plate,

$$\dot{m}_1\, C(T_o - T_{ol}) + \dot{m}_2\, C(T_o - T_A) = h_{cja2}\,(T_j - T_{a2}) + h_{CPa2}\,(T_P - T_{a2}) \qquad (6)$$

From equation (2) to (6) we get,

$$T_{a1} = \frac{T_A + T_{ol}}{2} \quad \text{and} \quad T_{a2} = \frac{T_i + T_o}{2}$$

$$T_i = \frac{\dot{m}_1 T_{ol} + \dot{m}_2 T_A}{\dot{m}_1 + \dot{m}_2} \qquad (7)$$

In addition,

$$h_{Pa2} = h_{Pj}\frac{(T_P - T_{ol})}{(T_P - T_{a2})} \qquad (8)$$

Average collector efficiency be,

$$\eta = \frac{(\dot{m}_1 + \dot{m}_2)C\,(T_o - T_A)}{I} \qquad (9)$$

Heat Transfer Coefficients [15]:

The convective heat transfer coefficient h_w, for air flowing over the outside surface of the glass cover depends on the wind velocity, V_W. Adams [20], is obtained the experimental result as,

$$h_{CS} = h_w + h_{rcs} \qquad (10)$$

$$h_w = 5.7 + 3.8\,V_w \qquad (11)$$

$$h_{rcs} = \varepsilon_c . \sigma\,(T_C^4 - T_S^4)\,(T_C - T_A) \qquad (12)$$

Neglecting the radiation heat transfer from cover to air

with, $T_S = (0.0552)\,(T_A)^{1.5}$ (13)

$$h_{PC} = h_{cPC} + h_{rPC} \qquad (14)$$

$$h_{cPC} = Nu_c \frac{k_a}{d} \qquad (15)$$

$$Nu_c = 0.093(Gr_c)^{0.31} \qquad (16)$$

and,

$$h_{rPC} = \frac{\sigma(T_P^2 + T_C^2)(T_P + T_C)}{\frac{1}{\varepsilon_P} + \frac{1}{\varepsilon_C} - 1} \qquad (17)$$

The average plate-to-jet air heat transfer coefficients [15] are

$$h_{Pj} = Nu_{Pj}\frac{k_a}{d} \qquad (18)$$

The forced convective heat transfer coefficients from jet plate to air above (h_{cja2}), from jet plate to air below (h_{cja1}) and from back plate to air (h_{cba1}) are written as,

$$h_{cja2} = \frac{A_e}{A} Nu_{ja2} \frac{k_a}{D_2} \quad (19)$$

$$Nu_{ja2} = 0.0293\,(Re_{ja2})^{0.8} \quad (20)$$

$$Re_{ja2} = \frac{(\dot{m}_1 + \dot{m}_2) L D_2}{Z_1\, \mu} \quad (21)$$

$$A_e = A - N\pi D^2 + 2N_1/N \quad (22)$$

$$h_{cja1} = \frac{A_e}{A} Nu_{ja1} \frac{k_a}{D_2} \quad (23)$$

$$Nu_{ja1} = 0.0293\,(Re_{ja1})^{0.} \quad (24)$$

$$Re_{ja1} = \frac{\dot{m}_1 L D_2}{Z_2\, \mu} \quad (25)$$

$$h_{cba1} = h_{cja1}\, A/A_e \quad (26)$$

The radiative heat transfer coefficient between the absorber and jet plate may be,

$$h_{rPj} = \frac{\sigma\left(T_P^2 + T_j^2\right)\left(T_P + T_j\right)}{\frac{1}{\varepsilon_P} + \frac{1}{\varepsilon_j} - 1} \quad (27)$$

Similarly, the radiative heat transfer coefficient between the absorber and jet plate can be written as,

$$h_{rjb} = \frac{\sigma\left(T_j^2 + T_b^2\right)\left(T_j + T_b\right)}{\frac{1}{\varepsilon_j} + \frac{1}{\varepsilon_b} - 1} \quad (28)$$

The bottom loss heat coefficient is calculated by using,

$$U_b = \frac{k_i}{l} \quad (29)$$

(Considering, heat loss from bottom is 0)

Calculation of friction factor

$$f_s = 0.085(Re_{ja2})^{-0.25} \quad \text{(Blassius equation)} \quad (30)$$

PARAMETRIC RANGE OF THE PRESENT STUDY

Parameters	Range
Z_1 / D	6.0 - 10.0
Z_2 / D	8.0 - 14.0
X / D	6.0 – 10.0
Re	3000 – 43000

RESULTS AND DISCUSSIONS

Variations of the outlet air temperature and collector efficiency (Cross and non - cross flow conditions) with mass flow rate of air:

Figs. 4 and 5 show that the outlet air temperature (T_o) decreases and the collector efficiency (η) increases with increase in mass flow rate of air. For X / D = 6.0 - 10.0, the outlet air temperature (T_o) of non - cross flow inline hole jet plate solar air heater is higher than non - cross flow staggered hole and cross-flow inline/staggered hole jet plate solar air heater. However, the collector efficiency (η) of cross - flow inline hole jet plate solar air heater for the same range is more than cross - flow staggered hole and non - cross flow inline/staggered hole jet plate solar air heater. The lower value of outlet air temperature for cross flow is due to deterioration of its degradation factor F_2. At $\dot{m}_1$ = 300 kg/ hm^2 and X / D = 10.0, the outlet air temperaure (T_o) in non - cross flow inline hole jet plate solar air heater has been found 2.4%, 2.7% and 3.45% higher than non - cross flow staggered, cross -flow inline and cross fow staggered hole jet plate solar air heater respectively. Whereas the collector efficiency (η) in cross-flow inline hole jet plate solar air heater is obtained 5.04%, 14.56% and 17.92% more than cross-flow staggered, non – cross flow inline and non-cross flow staggered hole jet plate solar air heater respectively. The present results (Figs. 4 and 5) reveals that the outlet air temperature (T_o) and collector efficiency (η) increases with decrease in jet hole diameter (D) resulting in higher outlet air temperature (T_o) and collector efficiency.

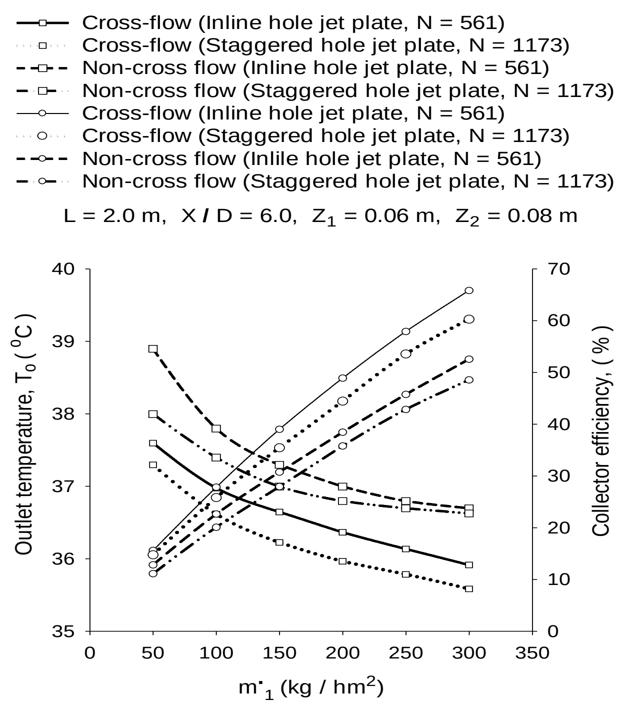

Fig. 4. Outlet air temperature and collector efficiency as function of mass flow rate of air ($\dot{m}_1$)

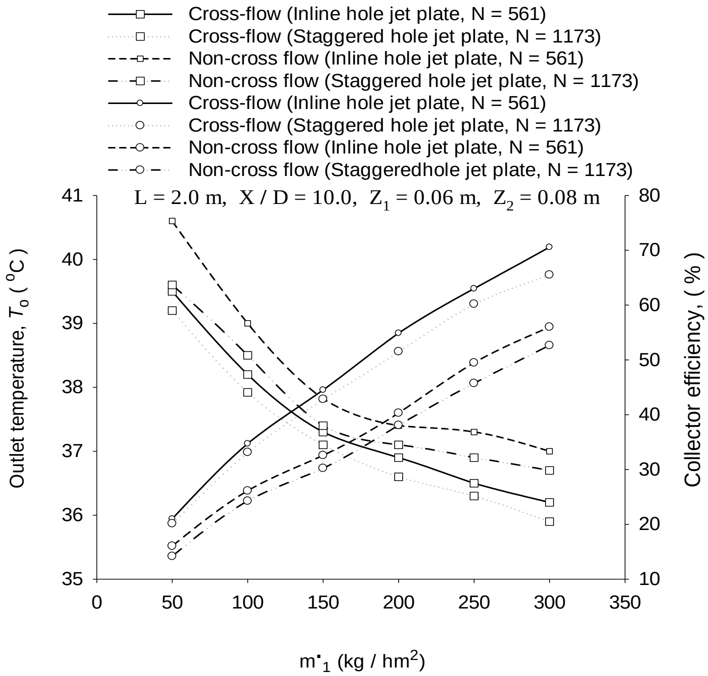

Fig. 5. Outlet air temperature and collector efficiency as function of mass flow rate of air ($\dot{m}_1$)

Effect of jet hole diameter on heat transfer coefficient of absorber plate to jet air and collector efficiency:

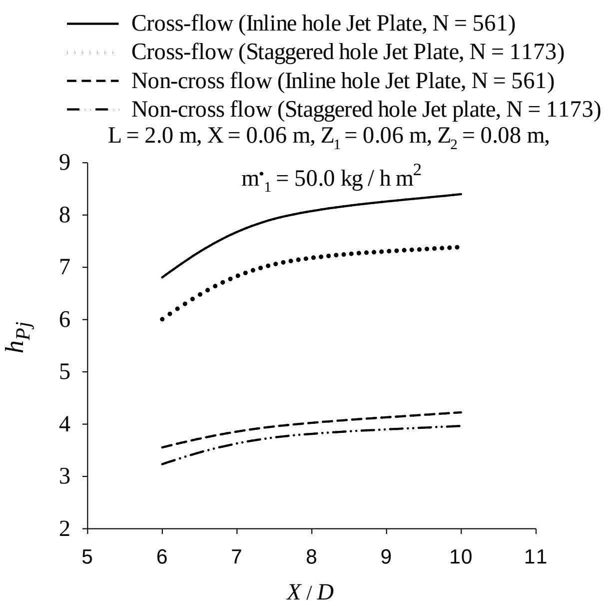

Fig. 6. Effect of jet hole diameter (D) on heat transfer coefficient (h_{Pj}) of absorber plate to jet air

Figs. 6 and 7 show the effect of jet hole diameter on heat transfer coefficient (h_{Pj}) of absorber plate to jet air and collector efficiency (η). These curves reveal that under both the cases h_{Pj} and η increase with decrease in jet hole diameter. It is observed that both h_{Pj} and η are increased with decreasing the size of the hole of the jet plate for fixed mass flow rate ($\dot{m}_1$) and the highest value of h_{Pj} and η are obtained at lowest jet plate hole diameter (D = 6.0 mm) because of getting higher velocity of jet air. The available literature [15] also shows the similar result in their presented work. For fixed mass flow rate ($\dot{m}_1$) and jet hole diameter (D), both h_{Pj} and η are observed higher in cross - flow inline hole jet plate solar air heater. At X / D = 10.0 and $\dot{m}_1$ = 50 kg/hm^2, the h_{Pj} and η of cross - flow inline hole jet plate solar air heater are found 49.6% and 30.84% higher as compare to non – cross flow inline hole jet plate solar air heater.

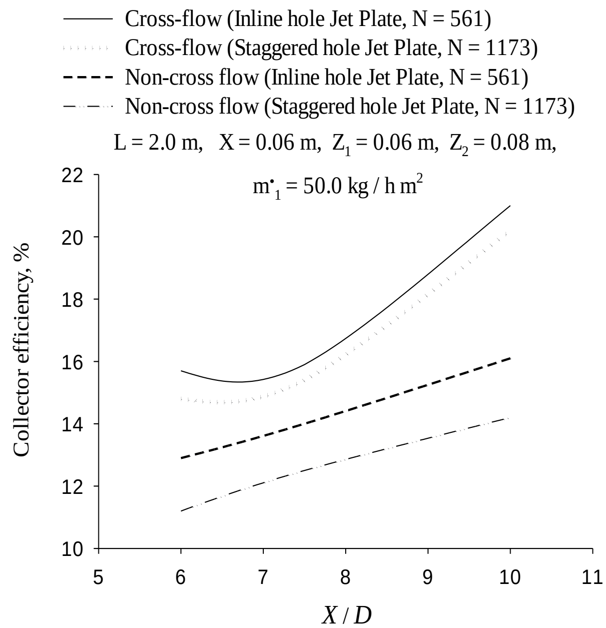

Fig. 7. Effect of jet hole diameter on Collector efficiency

Effect of the jet hole diameter on Nusselt number (Nu):

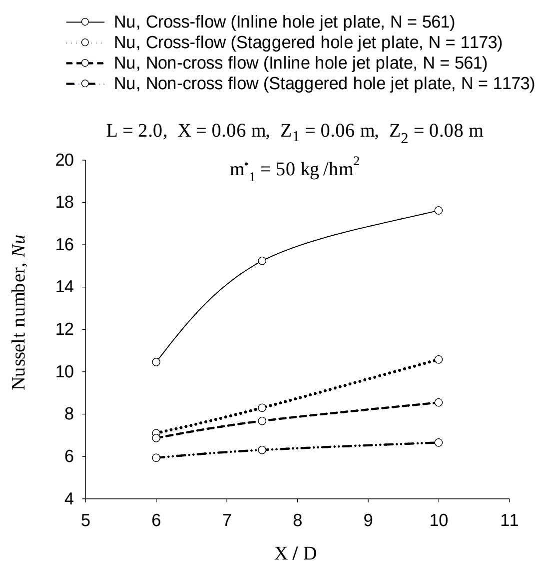

Fig. 8 (i)

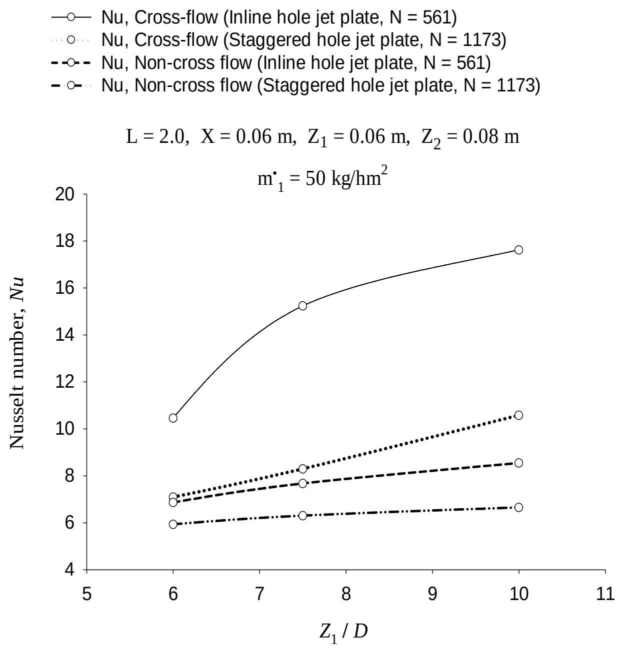

Fig. 8 (ii)

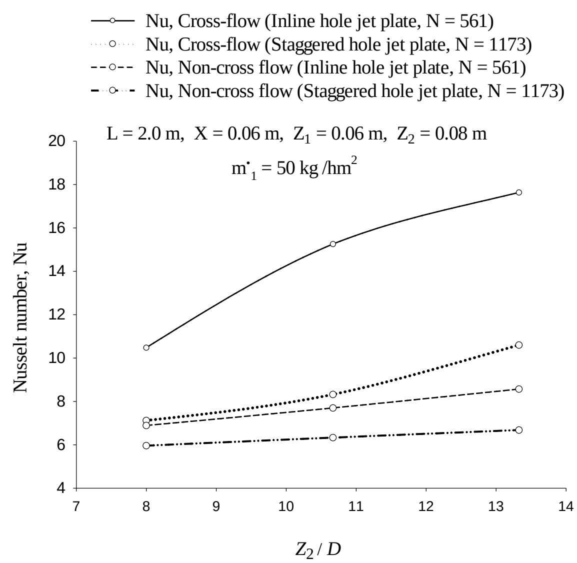

Fig. 8 (iii). Effect of jet hole diameter (D) on Nusselt number (Nu) and jet Reynolds number (Re_D)

Figs. 8(i-iii) show that the Nusselt number (Nu) increases with decrease in jet hole diameter (D) for fixed mass flow rate. For $\dot{m}_1$ = 50 kg/hm^2, X / D = 6.0 – 10.0, Z_1 / D = 6.0 – 10.0 and Z_2 / D = 6.0 – 10.0, the Nusselt number in cross-flow inline hole jet plate solar air heater is higher than cross-flow inline and non- cross flow inline/staggered hole jet plate solar air heater.

Variation of friction factor with Reynolds number:

For $\dot{m}_1$ = 50 - 300 kg/hm^2 and X / D = 6.0, the variation of friction factor (f_s) as a function of Reynolds number (Re) under cross-flow and non - cross flow inline/staggered hole jet plate solar air heater are shown in figs. 9 and 10. Under both the cases, curves indicate that friction factor (f_s) decreases with increase in Reynolds number. It is found that the value of gradient of curve in case of cross - flow condition is lower as compare to non- cross flow condition. For fixed mass flow rate ($\dot{m}_1$) and Re = 13000 - 43000, the friction factor (f_s) in non-cross flow condition is higher than cross-flow condition.

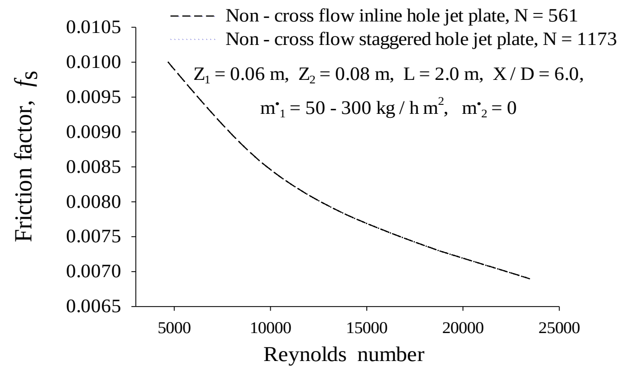

Fig. 9. Variation of f_S with Re for non-cross flow (Inline and Staggered hole)

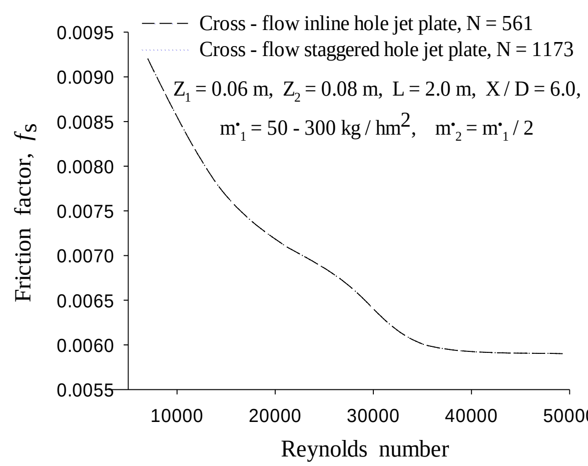

Fig. 10. Variation of f_S with Re for cross-flow (Inline and Staggered hole)

CONCLUSION

Based on the above results, the following conclusions are made as given below:

At fixed mass flow rate ($\dot{m}_1$) and jet hole diameter (D), the heat transfer coefficient (h_{Pj}) of absorber plate to jet air, Nusselt number (Nu) and collector efficiency (η) are higher in cross - flow inline hole jet plate solar air heater than cross - flow staggered hole and non - cross flow inline/staggered hole jet plate solar air heater. The outlet air temperature (T_o) decreases and the collector efficiency (η) increases with increase in mass flow rate of air. The friction factor decreases with increase of Reynolds number. For $\dot{m}_1$ = 50 - 300 kg/hm^2, X / D = 6.0, the friction factor (f_s) has been found more in non - cross flow inline/staggered hole than cross - flow inline/staggered hole jet plate solar air heater.

REFERENCES

[1] Thombre S. B, Sukhatme S. P,. Turbulent flow and friction factor characteristics of shrouded fin arrays with uninterrupted fins. Experimental Thermal and Fluid Science, 1995; 10, 338

[2] Karsli S,. Perfomance analysis of new design solar air collectors for drying applications. Renewable Energy 2007; 32 (10), 1645-1660 doi:10.1016 / j.renene. 2006.08.005.

[3] Romdhane B. S. The air solar collectors:Comparative study, introduction of baffles to favor the heat transfer. Solar Energy 2007; 81 (1), 139-149. doi: 10. 1016/j.solener.2006. .05.002.

[4] Akpinar E. K, Kocyigit F,. Experimental investigation of thermal performance of solar air heater having different obstacles on absorber plates. Int common Heat Mass 2010; 37 (4), 416-421.

[5] Omojaro A, Aldabbagh L,. Experimental performance single and double pass solar air heater with fins and steel wire mesh as absorber. Applied Energy 2010; 87 (12), 3759-3765. doi:10.1016 / j.apenergy. 06. 020.

[6] Seluk M. K,. Solar air heaters and their applications. Academic Press 1977; New York.

[7] Tan H. M, Charters W. W. S,. Experimental investigation of forced convective heat transfer for fully developed turbulent flow in a rectangular duct with asymmetric heating. Solar Energy 1970; 13 (1), 121-125.

[8] Close, D. J., Dunkle, R. V., 1976. Behaviour of adsorbent energy storage beds. Solar Energy 18 (4) 287-292.

[9] Liu C. H, Sparrow E. M,. Convective - radiative interaction a parallel plate channel application to air operated solar collectors. Int. J, Heat Mass Transfer 1980; 23 (8), 1137-1146.

[10] Duffie J. A, et al,. Solar engineering 2nd edition 1978; Mc Graw-Hill, New York.

[11] Kreith F, Kreider J. F,. Principles of solar engineering 2nd Edition 1980; Mc Graw -Hill, New-York.

[12] Tonui J. K, Tripanagnostopoulos Y,. Improved pv/t solar collectors with heat extraction by forced or natural air circulation. Renew. Energy 2007; 32 (4), 623-637.

[13] Gao W, Lin W, Liu T, Xia C,. Analytical and experimental studies on the thermal performance of cross-corrugated and flate-plate solar air heaters. Applied Energy 2007; 84 (4), 425-441.

[14] Mohamad A. A,. High efficiency solar air heater. Solar Energy 1997; 60 (2), 71-76.

[15] Choudhury C, Garg H. P,. Evaluation of a jet plate solar air heater. Solar Energy 1991; Vol. 46, No. 4, pp. 199-209.

[16] Singh S. N,. Performance studies on continuous longitudinal fins solar air heater. Journal of ISM Dhanbad 2006; vol. 2.

[17] Irfan Kurtbas,. Experimental investigation of solar air heater with free and fixed fins. Int. J. of Science and Technology 2006; Volume 1, No 1, 75-82.

[18] Belusko M, Saman W, Bruno F,. Performance of jet impingement in unglazed air collector Solar Energy 2008; 82, 389 - 398.

[19] Chauhan Ranchan, Thakur N. S,. Heat transfer and friction factor correlation for jet impingement in solar air heater. Experimental Thermal and Fluid Science 2013; 44, 760-767.

[20] Adams W. A. Mc,. Heat transmission. 3rd edition 1954; Mc Graw-Hill, New York, p. 249.